Polyoctahedral Silsesquioxane–Nanoparticle Electrolytes for Lithium Batteries: POSS–Lithium Salts and POSS–PEGs

ARTICLE *in* CHEMISTRY OF MATERIALS · NOVEMBER 2011

Impact Factor: 8.35 · DOI: 10.1021/cm2015675

2 AUTHORS:

Parameswara Rao Chinnam
Temple University
10 PUBLICATIONS **41** CITATIONS
SEE PROFILE

Stephanie L Wunder
Temple University
92 PUBLICATIONS **1,652** CITATIONS
SEE PROFILE

CHEMISTRY OF MATERIALS

Article

pubs.acs.org/cm

Polyoctahedral Silsesquioxane-Nanoparticle Electrolytes for Lithium Batteries: POSS-Lithium Salts and POSS-PEGs

Parameswara Rao Chinnam and Stephanie L. Wunder*

Department of Chemistry, Temple University, Philadelphia, Pennsylvania 19122, United States

Supporting Information

ABSTRACT: Nanocomposite electrolytes have been prepared from mixtures of two polyoctahedral silsesquioxanes (POSS) nanomaterials, each with a $SiO_{1.5}$ core and eight side groups. POSS-PEG_8 has eight polyethylene glycol side chains that have low glass transition (T_g) and melt (T_m) temperatures and POSS-benzyl$_7$(BF_3Li)$_3$ is a Janus-like POSS with hydrophobic phenyl groups and −Si−O−BF_3Li ionic groups clustered on one side of the $SiO_{1.5}$ cube. The electron-withdrawing POSS cage and BF_3 groups enable easy dissociation of the Li^+. In the presence of polar POSS-PEG_8, the hydrophobic phenyl rings of POSS-benzyl$_7$(BF_3Li)$_3$ aggregate and crystallize, forming a biphasic morphology, in which the phenyl rings form the structural phase and the POSS-PEG_8 forms the conductive phase. The −Si−O−BF_3− Li^+ groups of POSS-benzyl$_7$(BF_3Li)$_3$ are oriented toward the polar POSS-PEG_8 phase and dissociate so that the Li^+ cations are solvated by the POSS-PEG_8. The nonvolatile nanocomposite electrolytes are viscous liquids that do not flow under their own weight. POSS-PEG_8/POSS-benzyl$_7$(BF_3Li)$_3$ at O/Li = 16/1 has a conductivity of $\sigma = 2.5 \times 10^{-4}$ S/cm at 30 °C, which is 17 times greater than that of POSS-PEG_8/$LiBF_4$, and a low activation energy ($E_a \sim 3-4$ kJ/mol); $\sigma = 1.6 \times 10^{-3}$ S/cm at 90 °C and 1.5×10^{-5} S/cm at 10 °C. The lithium ion transference number was $t_{Li^+} = 0.50 \pm 0.01$, as a result of the reduced mobility of the large, bulky anion, and the system exhibited low interfacial resistance that stabilized after 3 days (both at 80 °C).

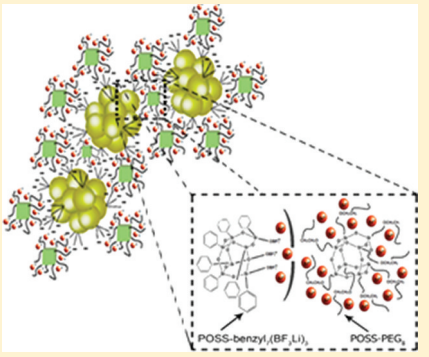

KEYWORDS: *batteries, lithium, silsesquioxanes, nanomaterials, solid polymer electrolytes, Janus nanoparticles*

INTRODUCTION

Electrical energy storage systems are currently used for powering portable electronic devices (such as phones and laptops), but they are increasingly required for future large battery applications, such as for plug-in hybrid vehicles/electric vehicles and for the storage of energy generated by the wind, the Sun, and nuclear fusion.[1] Because rechargeable (secondary) lithium and lithium ion batteries have some of the highest energy storage capabilities, there has been extensive research to improve their energy density, power density, and safety, as risks increase with the size of the energy-storage device.[1] Failure mechanisms and safety hazards in lithium and lithium ion batteries arise as a result of the development of shorts between the anode and cathode after many charge/discharge cycles, as the result of lithium dendrite formation (when lithium metal is used) and the presence of both a combustible material and an oxidizing agent, which can result runaway reactions and fires or explosions.[2,3]

There is a continual compromise between the high conductivity that can be achieved using flammable liquid electrolytes, with the associated safety concerns, and the improved safety (no leakage, reduced dendrite growth) and mechanical properties achieved with solid polymer electrolyes (SPEs), which have the drawback of reduced conductivity and charge/discharge rates.[4−6] There have been many attempts to increase the conductivity of SPEs, in particular, to achieve high room temperature (RT) conductivities. The most investigated SPE, poly(ethylene oxide) (PEO), has poor conductivity, especially below the melt temperature (~65 °C) and slow charge/discharge rates, because conduction occurs through a mechanism that is associated with the slow dynamics of polymer backbone motions rather than the diffusion of ions through a liquid.[6] Further, the lithium ion transference number is low (0.2−0.4),[7] with the higher numbers achieved by the addition of ceramic nanoparticles,[8,9] which can lead to concentration polarization that limits the power delivery of the battery.[10]

Attempts to increase conductivity have included the addition of inorganic nanoparticles.[8,11] Lower glass transition temperatures (T_g) can lead to increased conductivities; therefore, side chain PEGs have been coupled to many backbone polymers.[6] Lastly, there have been many attempts to synthesize so-called single ion conductors, where the anion is tethered to the polymer chain, thus avoiding concentration polarization effects. However, this approach often depresses the overall electrolyte conductivity, while increasing t_{Li^+} to values approaching 1.[12]

Attempts to increase RT conductivity of liquid electrolytes while decreasing their volatility have included the development/use of ionic liquids (ILs), which have T_m below ~100 °C, ultralow vapor pressure, high thermal stability, wide redox

Received: June 3, 2011
Revised: October 21, 2011

dx.doi.org/10.1021/cm2015675|*Chem. Mater.* XXXX, XXX, XXX−XXX

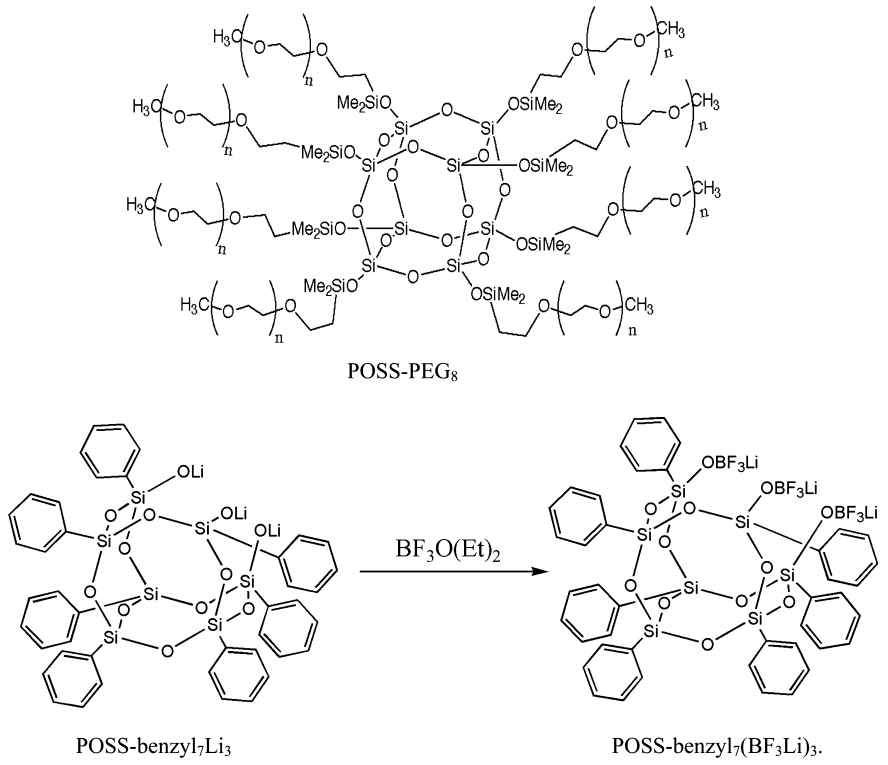

Figure 1. Structures of POSS-PEG_8, POSS-benzyl$_7$$Li_3$ and POSS-benzyl$_7$$(BF_3Li)_3$.

windows, and high RT conductivity.[13] However, similar to the case of other liquid electrolytes, ILs did not suppress dendrite growth and had low Li^+ transference numbers (0.05).[14] Tethering of ionic liquids (ILs) to zirconia nanoparticles was proposed to mitigate the deficiencies of ILs and improve their mechanical properties.[15] These IL-nanoscale ionic materials (IL-NIMS) doped with lithium bis(trifluoromethylsulfonyl) imide (LiTFSI) salt exhibited redox stabilities of 4.3 V, thermal stabilities greater than 400 °C, Li transference numbers of 0.35, long-term interfacial stability (using a lithium anode), and RT conductivities of $\sim 10^{-4}$ S/cm.[15] RT-ILs synthesized from polyoctahedral silsesquioxane (POSS)-octacarboxy anions $(POSS\text{-}COO^-)_8$ and the imidazolium cation have been reported.[16] POSS nanoparticles are hybrid inorganic/organic nanoparticles with a $SiO_{1.5}$ silicon−oxygen framework and eight attached organic moieties. Other approaches to increase RT conductivities of liquid electrolytes include the synthesis of colloidal silica (SiO_2) (or other inorganic) nanoparticles, to which PEG oligomers were grafted, referred to as nanoscale organic hybrid materials (NOHMs),[17] and POSS with eight attached PEG side chains $(POSS\text{-}PEG)_8$.[18−20] The NOHMS and POSS-PEG_8 electrolytes were nonvolatile, exhibited RT conductivities of $\sim 10^{-4}$ S/cm upon the addition of low molecular weight lithium salts, and had high thermal stabilities (to ~400 °C); the NOHMs had large electrochemical stability windows (0.5−5 V versus Li).

There is thus a need to develop nonflammable electrolytes with both high conductivities and high t_{Li^+} that can be used with separators, incorporated into polymers as gels, or as the polymer electrolytes themselves. In general, the factors that increase conductivity are lower T_g and larger and more stable anions, so that Li^+ can more easily dissociate. There is evidence that, in block copolymers, where one block provides the conduction path and one provides the structural component, the microphase separated morphology can be engineered to enhance conductivity. In particular, increased salt dissociation can occur if the anions and cations are partitioned between the two phases,[21,22] highlighting the impact of nanoscale morphology on the electrolyte performance.

Here, we present a new nanoparticle system composed of mixtures of POSS-PEG_8 and POSS-Li salt functionalized nanoparticles, for use as electrolytes in lithium batteries. POSS-PEG_8, a polyoctahedral silsesquioxane functionalized with eight PEG, $-(CH_2CH_2O)_m-$, chains ($m \sim 13.3$) is shown in Figure 1. The other component in the system, a newly synthesized multi-ionic lithium salt, POSS-benzyl$_7$$(BF_3Li)_3$, made by reaction of POSS-benzyl$_7$$Li_3$ with $BF_3(OC_2H_5)_2$ (Figure 1), has Janus-like properties, with one end predominantly hydrophobic and the other end ionic in character. It has been suggested that bifunctionalized polyoctahedral silsesquioxanes can provide Janus-like behavior, because side arms with similar functionality or properties (e.g., hydrophobicity, polarity) are statistically likely to segregate to opposite sides of a cubically symmetric POSS during synthesis.[23] Because these POSS have cubic symmetry, there will be one face where three or four of the same group will be found[23] and where, during synthesis, ordering of side chains has been observed experimentally.[24,25] In the current investigation, the electrochemical properties and morphology of mixtures of hydrophilic POSS-PEG_8 with the Janus-like POSS-benzyl$_7$$(BF_3Li)_3$ were investigated.

EXPERIMENTAL SECTION

Materials. Trilithium-1,3,5,7,9,11,14-heptaphenyltricyclo [7.3.3.1-(5,11] heptasiloxaneendo-3,7,14 trisilanolate (product no. SO1457), also known as trisilanolphenyl POSS lithium salt ($C_{42}H_{35}Li_3O_{12}Si_7$, MW = 949.15 g/mol, soluble in methylene chloride), and polyethylene glycol POSS (product no. PG1190), with a chemical formula $(C_{2m+3}H_{4m+7}O_{m+1})_n(SiO_{1.5})_n$ and n = 8, 10, 12 and $m \sim 13.3$ and

dx.doi.org/10.1021/cm2015675 | Chem. Mater. XXXX, XXX, XXX−XXX

MW = 5576.6 (for n = 8), were gifts from Hybrid Plastics (Hattiesburg, MS). Their chemical structures (Figure 1) will be referred to as POSS-benzyl$_7$Li$_3$ and POSS-PEG$_8$. Dichloromethane (CH_2Cl_2), acetonitrile (CH_3CN), deuterated acetonitrile (CD_3CN), trifluoride diethyl etherate, $BF_3(OC_2H_5)_2$ $LiBF_4$, tetrahydrofuran (THF), and polystyrene (PS) (MW = 80 000 g/mol) were obtained from Sigma-Aldrich (St. Louis, MO). PS-*b*-PEO (PS: 384 000 g/mol; PEO: 8000 g/mol) was purchased from Polymer Source, Inc. (Montreal, Quebec). Before use, dichloromethane was passed through two columns of neutral alumina and stored over molecular sieves in an MBRAUN Lab Master 130 (MBRAUN U.S.A., Stratham, NH) glovebox purged with argon.

Synthesis of POSS-benzyl$_7$(BF$_3$Li)$_3$. POSS-benzyl$_7$Li$_3$ (Figure 1) was dried in a vacuum oven at 80 °C for 34 h and then dissolved in dry dichloromethane. A stoichiometrically equivalent amount of $BF_3(OC_2H_5)_2$ was added to the POSS-benzyl$_7$Li$_3$ in an argon atmosphere at 25 °C. The reaction mixture was stirred for 1 h. A white powder was observed to settle at the bottom of the reaction mixture. The powder was filtered and washed four times with a large excess of dichloromethane and dried in a vacuum oven at 80 °C for 24 h. The resultant powder was hydroscopic, and it was stored in the glovebox under an argon atmosphere.

To help with the F-NMR (fluorine NMR) and FTIR (Fourier transform infrared spectroscopy) characterizations of the product and to determine if all three lithium atoms on the POSS-benzyl$_7$Li$_3$ could be substituted with $-BF_3Li$, the same reaction was carried out with $^1/_3$ and $^2/_3$ stoichiometry (i.e., just enough $BF_3(OC_2H_5)_2$ to react with 1 and 2 of the lithiums), as well as a stoichiometric excess of $BF_3(OC_2H_5)_2$.

Preparation of Mixtures of POSS-PEG$_8$ with POSS-benzyl$_7$(BF$_3$Li)$_3$, POSS-benzyl$_7$Li$_3$ and LiBF$_4$. POSS-PEG$_8$ with POSS-benzyl$_7$Li$_3$ was prepared by dissolution of dried (90 °C, 2 days, vacuum) POSS-benzyl$_7$Li$_3$ in anhydrous dichloromethane, followed by the addition of a calculated amount of the POSS-benzyl$_7$Li$_3$ dichloromethane solution to dried (90 °C, 2 days, vacuum) POSS-PEG$_8$ and the removal of the dichloromethane at 60 °C under vacuum for 24 h. The amount of added salt was based on the number of $-(CH_2CH_2O)_n-CH_3$ in POSS-PEG$_8$.

POSS-PEG$_8$ with POSS-benzyl$_7$(BF$_3$Li)$_3$ was prepared by physically mixing dry (90 °C, 2 days, vacuum) POSS-benzyl$_7$(BF$_3$Li)$_3$ with dry (90 °C, 2 days, vacuum) POSS-PEG$_8$. The mixture was stirred in an argon atmosphere at 100 °C until a slurry formed. The slurry was reheated in a vacuum oven overnight. A sample (O/Li = 16/1) prepared by the co-dissolution of POSS-PEG and POSS-benzyl$_7$(BF$_3$Li)$_3$ in acetonitrile had the same conductivity after evaporation of the solvent as samples prepared without solvent. SPEs were formed by co-dissolution of polystyrene (PS), PS(384 000)-*b*-PEO(8000), POSS-PEG$_8$ with POSS-benzyl$_7$(BF$_3$Li)$_3$ in toluene, followed by solvent evaporation.

POSS-PEG$_8$ with $LiBF_4$ was prepared by physically mixing dry (70 °C, 1 day, vacuum) $LiBF_4$ with dry (90 °C, 2 days, vacuum), stirred at 80 °C in an argon atmosphere until a homogeneous mixture formed, and then reheated under vacuum overnight.

Characterization. *Calorimetry.* Differential scanning calorimetry (DSC), using a TA Instruments Hi-Res DSC 2920 (TA Instruments, New Castle, DE) at 10 °C/min under N_2, was used to measure phase transition temperatures. Data are reported for the second heating cycles. Thermogravimetric analysis (TGA) data, to determine the degradation temperatures of the components and mixtures, was obtained on a TA Instruments Hi-Res TGA 2950 (TA Instruments, New Castle, DE) with a ramp rate of 10 °C/min. Samples of approximately 10−15 mg were placed in the sample pans and heated from ambient temperature to 800 °C. Nitrogen was used as a purge gas at a flow rate of 60 mL/min.

Spectroscopy. Fourier transform infrared spectroscopy (FTIR) of the POSS-benzyl$_7$(BF$_3$Li)$_3$ and POSS-benzyl$_7$Li$_3$ were obtained by attenuated total reflection (ATR), with 200 scans and a resolution of 4 cm^{-1}, using a Nicolet 580 research FTIR with a Specac Golden Gate ATR accessory (diamond lens) equipped with an MCT detector. ^{19}F-NMR spectra were obtained on a 400 MHz Bruker Biospin AVANCE 400 (Billerica, MA), using trichlorofluoromethane as the internal calibration solvent. CD_3CN and CD_2Cl_2 were used as the solvents for POSS-benzyl$_7$(BF$_3$Li)$_3$ and POSS-benzyl$_7$Li$_3$, respectively.

High resolution mass spectroscopy (HRMS) data were acquired on a Waters (Milford, MA) LC-TOF (liquid chromatography time of flight) mass spectrometer (model LCT-XE Premier), using electrospray ionization in positive or negative mode, depending upon the analyte. The sample was prepared in 100% methanol and introduced using flow injection through a Waters Alliance separation module 2695 into a mobile phase of 100% methanol (flow rate of 0.25 mL/minute). Leucine enkephalin (Waters) was used as an internal reference (2 ng/μL in 1:1 v/v acetonitrile/water mixed in equal parts with 1% acetic acid in 1:1 v/v acetonitrile/water) and introduced by infusion. Data analysis was performed using the automated Waters software and the mass calculated from the molecular ion formula.

Electrochemical Testing. Ionic conductivities were measured by AC impedance spectroscopy using a Schlumberger HF frequency response analyzer (model SI 1255) in combination with a PAR model 273A EG&G Princeton Applied Research (Oak Ridge, TN) potentiostat/galvanostat in the frequency range 0.01−100 kHz. Control of the equipment was through Z-Plot electrochemical software (Scribner Associates, Inc., Southern Pines, NC). Temperature dependent conductivities were obtained in an electrochemical cell using stainless steel blocking electrodes with (for $LiBF_4$) or without (for POSS-benzyl$_7$Li$_3$ and POSS-benzyl$_7$(BF$_3$Li)$_3$) a polypropylene (PP) separator (Celgard 2400 25 μm microporous monolayer membrane, PP, Celgard, Charlotte, NC).

Conductivity data were obtained from the impedance spectra, which were slanted lines at high temperatures/conductivities, and consisted of depressed semicircles at higher frequencies and slanted lines at lower frequencies at low temperatures/conductivities. The resistance (R) was obtained from the intercept of the slanted line extrapolated to the real axis of plots of the imaginary (Z'') vs real (Z') components of the impedance spectra. The specific ionic conductivity (σ) was obtained from $\sigma = t/AR$, where R is the resistance (Ω), A = area (1 cm^2) of the stainless steel electrodes, and t = thickness of the film (cm), which was 25 μm for POSS-PEG$_8$/$LiBF_4$ and 0.3 mm for POSS-PEG$_8$/POSS-benzyl$_7$(BF$_3$Li)$_3$ and POSS-PEG$_8$/POSS-benzyl$_7$Li$_3$.

For POSS-PEG$_8$/POSS-benzyl$_7$(BF$_3$Li)$_3$ and POSS-PEG$_8$/POSS-benzyl$_7$Li$_3$, the electrolyte was kept directly between the stainless steel electrodes, constrained using a 0.3 mm thick Teflon O-ring (1 cm^2 enclosed area). The cell was annealed overnight at 90 °C in a gas chromatography (GC) oven, checked for leaks (very rare), followed by temperature dependent conductivity runs, and rechecked for leaks following the runs. Conductivity measurements were first made on the cooling cycle. The sample was then reheated and conductivity measurements obtained, confirming that the heating and cooling cycles had the same values of σ. At each temperature, the sample was equilibrated for about 30 min, until the resistance measurements responded to small (~1 °C) temperature perturbations. The resistances measured on the heating and cooling cycles were very close. Below room temperature, the GC oven was cooled with dry ice, and the conductivity data were obtained on the heating cycle.

Lithium ion transport numbers and interfacial resistance values were obtained using the same cell as that for ionic conductivities but with symmetric nonblocking lithium electrodes (0.38 mm thick). Interfacial stability was investigated by measuring the time-dependent impedance at 80 °C under open circuit potential. The lithium ion transference number (t_{Li^+}), the fraction of the charge carried by the cations, was also measured at 80 °C and calculated using[26,27]

$$t_{Li^+} = I_{ss}(\Delta V - I_0R_0)/I_0(\Delta V - I_sR_{ss}) \quad (1)$$

A DC pulse (ΔV) of 50 mV was used to polarize the cell, and the initial current, I_0, and final, steady state, I_{ss}, values measured. Impedance spectra were measured initially and at steady state to obtain the resistances R_0 and R_{ss}, respectively, at 80 °C.

dx.doi.org/10.1021/cm2015675 | Chem. Mater. XXXX, XXX, XXX−XXX

RESULTS AND DISCUSSION

The motivation for preparing mixtures of POSS functionalized nanoparticles, in this case POSS-PEG_8 and POSS-Li salts, was that both components had desirable characteristics that could contribute to enhanced electrochemical and mechanical properties for the composite electrolyte. POSS-PEG_8 has a large number of chain ends that increase the free volume, and the short chain length of the arms results in a decreased T_m of close to 0 °C,[18] significantly less than that of high molecular weight PEO (~65 °C). At high temperatures (>~60 °C), conductivities of POSS-PEG_8/$LiBF_4$, as well as POSS-PEG_8 with other lithium salts ($LiClO_4$, $LiN(CF_3CF_2SO_2)_2$, $LiN(CF_3SO_2)_2$, $LiCF_3SO_3$, $LiPF_6$, $LiAsF_6$),[19] were comparable to those observed for linear PEG (MW = 500 g/mol) and high molecular weight PEO with the same Li salts,[28] indicating that there is the same conduction mechanism for PEO and POSS-PEG_8, namely, one in which Li^+ mobility is coupled to backbone motions of the chains. However, at low temperatures, the conductivity of POSS-PEG_8/Li salt is significantly higher than for PEO/Li salt, as crystallization is reduced or eliminated in the former case.

The motivation for the synthesis and use of the Li salt POSS-benzyl$_7$(BF_3Li)$_3$, were 3-fold. First, it was suspected that not all of the Li^+ in the commercially available POSS-benzyl$_7$$Li_3$ would dissociate or be very soluble in typical (ethylene carbonate, diethyl carbonate, dimethylcarbonate, EC/DEC/DMC) aprotic solvents used in lithium ion rechargeable batteries. Therefore, a reaction for the conversion of COO-Li^+ to $COOBF_3Li^+$, namely, complexation through the addition of the Lewis acid boron trifluoride (BF_3), was attempted on POSS-benzyl$_7$$Li_3$ in order to convert Si−O^-Li^+ to the more dissociative Si−O−$BF_3^-Li^+$. This approach, the direct addition of stoichiometric amounts of BF_3 to polymer gel electrolytes, has been used successfully on Li carboxylates.[29−31] The addition of BF_3 was also suggested to form a passivation layer on the lithium electrode that inhibited reaction between lithium and the solvent,[29] helped form protective layers that slowed down the growth of highly resistive interfaces,[30] and slightly improved the electrochemical stability of PEO/poly(lithium carboxylate)s.[32]

Second, the proposed POSS-benzyl$_7$(BF_3Li)$_3$ compound is the precursor of Janus-like POSS Li salts, with one end of the molecule very hydrophobic, as a result of the seven benzyl groups, and the other end highly ionic, as a result of the three Si−O−$BF_3^-Li^+$. As shown in Figure 1, this material is not a true Janus particle, because the −BF_3Li are separated by phenyl groups. However, true Janus structures can be formed with incompletely condensed half phenyl and half sodium salts,[33] and it has been suggested that bifunctionalized polyoctahedral silsesquioxanes can provide Janus-like behavior, because side arms with similar functionality or properties (e.g., hydrophobicity, polarity) are statistically likely and they have been observed to segregate to opposite sides of a cubically symmetric POSS during synthesis.[23−25] Thus, although POSS-benzyl$_7$(BF_3Li)$_3$ is not a true Janus structure, its behavior in mixed nanocomposite systems can demonstrate whether this approach is viable for nanocomposite electrolytes.

Lastly, the POSS-benzyl$_7$(BF_3Li)$_3$ is a large, bulky anion, with an electron-withdrawing $SiO_{1.5}$ cage, which might be expected to enhance the lithium ion transference number.

Here, we hypothesized that mixtures of Janus-like POSS-benzyl$_7$(BF_3Li)$_3$ and polar POSS-PEG_8 would form a phase separated morphology in which the phenyl groups segregated together and contained the dissociated Si−O−BF_3^- anion. The Li^+ cations could then be solvated in the polar POSS-PEG_8 phase. Because the nanocomposite electrolyte was expected to be nonvolatile, it could be used by itself or eventually incorporated into a polymer, either by blending or copolymerization, to yield a solid polymer electrolyte.

The first step toward this goal was the modification of the precursor salt, POSS-benzyl$_7$$Li_3$, to form POSS-benzyl$_7$($BF_3Li$)$_3$. Unlike POSS-benzyl$_7$$Li_3$, the final product was soluble in polar solvents, indicating enhanced dissociation of the Li^+. The reverse, namely, the weak dissociation of POSS-benzyl$_7$$Li_3$ was evidenced by its solubility in nonpolar solvents, as a result of the seven aromatic benzene rings. A table of solubilities for POSS-PEG_8, POSS-benzyl$_7$$Li_3$ and POSS-benzyl$_7$(BF_3Li)$_3$ is given in the Supporting Information. FTIR data (Figure 2) show both POSS-benzyl$_7$$Li_3$ and POSS-benzyl$_7$(BF_3Li)$_3$ in the spectral region 1200 to 1900 cm^{-1}. The vibration at 1637.8 cm^{-1} dominates the spectrum of the POSS-benzyl$_7$(BF_3Li)$_3$ but is absent for POSS-benzyl$_7$$Li_3$. It is attributed to a Si−O−BF_3−Li asymmetric stretching mode, in analogy with similar results observed for the 1640 cm^{-1} vibration that has been identified as the asymmetric stretching vibration of $COOBF_3$−Li.[22,30]

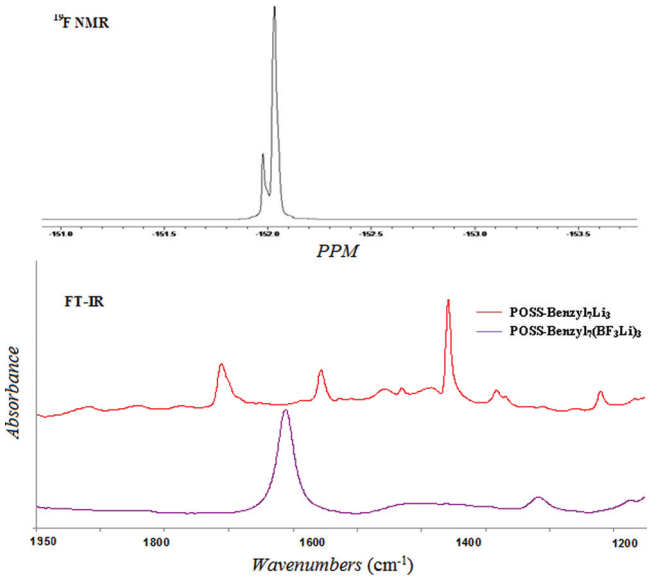

Figure 2. FTIR spectra (bottom) of POSS-benzyl$_7$$Li_3$ and POSS-benzyl$_7$(BF_3Li)$_3$ showing appearance of the −Si−O−BF_3Li groups after treatment with $BF_3(OC_2H_5)_2$; ^{19}F-NMR spectra (top) of POSS-benzyl$_7$(BF_3Li)$_3$; minor peak is POSS-benzyl$_7$Li(BF_3Li)$_2$.

To determine how many of the Si−O−Li groups reacted with the $BF_3(OC_2H_5)_2$ to form Si−O−BF_3Li, we analyzed samples synthesized with an amount of etherate necessary for the substitution of 1, 2, and 3 of the Si−O−Li groups. Samples prepared with 3 equiv were directly soluble in acetonitrile, but those prepared with 1 and 2 equiv were not. However, after extensive rinsing with dichloromethane, these materials were soluble in acetonitrile. The results indicate that the POSS lithium salts with 1 or 2 equiv were mostly removed with dichloromethane. NMR data of the rinsed material (Figure 2) show a major peak at 152.05 ppm, which we attribute to the POSS-benzyl$_7$(BF_3Li)$_3$, and a smaller peak at 151.95, attributed to POSS-benzyl$_7$Li(BF_3Li)$_2$. No NMR peaks from the $BF_3(OC_2H_5)_2$ (151.35 ppm) were observed. LC-MS data, in

dx.doi.org/10.1021/cm2015675 | Chem. Mater. XXXX, XXX, XXX−XXX

Table I. Glass Transition Temperatures (T_g), Melt Temperatures (T_m), and Conductivity (σ) of POSS-benzyl$_7$(BF$_3$Li)$_3$, POSS-benzyl$_7$Li$_3$ and LiBF$_4$ in POSS-PEG$_8$, as a Function of O/Li, Molarity (M) at 10, 30, and 90 °C, and Parameters (E_a, A) of Fit to the Vogel−Tammann−Fulcher (VTF) Equation

					σ, S/cm				
	O/Li	M, moles Li$^+$/L	T_g, °C	T_m, °C	90 °C	30 °C	10 °C	E_a, kJ/mol	A
POSS-PEG$_8$			−81	−2.0					
POSS-benzyl$_7$(BF$_3$Li)$_3$	20/1	0.95	−46.5		8.21×10^{-4}	1.04×10^{-4}	1.62×10^{-5}	3.4	3.3
	18/1	1.1	−44.4		1.09×10^{-3}	1.00×10^{-4}	1.85×10^{-5}	3.6	5.7
	16/1	1.2	−39.1		1.61×10^{-3}	2.50×10^{-4}	5.52×10^{-5}	2.8	3.1
	14/1	1.4	−38.4		7.14×10^{-4}	3.97×10^{-5}	4.20×10^{-6}	4.1	9.4
	12/1	1.6	−37.7		6.46×10^{-4}	1.51×10^{-5}	1.95×10^{-6}	4.7	22.0
	10/1	1.9	−35.3		7.16×10^{-4}	3.57×10^{-5}	4.44×10^{-6}	4.0	9.7
	8/1	2.4	−30.0		1.27×10^{-3}	1.03×10^{-4}	2.3×10^{-5}	2.9	3.2
	6/1	3.2	−8.0		5.25×10^{-6}				
LiBF$_4$	16/1	1.2	−63.6		1.08×10^{-4}	1.50×10^{-5}	5.92×10^{-6}	4.3	0.33
	12/1	1.6	−53.0		1.00×10^{-4}	8.09×10^{-6}	1.87×10^{-6}	4.3	1.1
	8/1	2.4	−48.3		1.85×10^{-4}	1.76×10^{-6}	2.46×10^{-6}	4.0	1.7
	6/1	3.2	−38.9		8.57×10^{-6}				
POSS-benzyl$_7$Li$_3$	16/1	1.2	−73.0	−7.8	2.20×10^{-5}	2.98×10^{-6}	9.06×10^{-7}	4.3	0.1
	12/1	1.6	−70.0	−5.3	1.29×10^{-5}	2.43×10^{-6}	8.45×10^{-7}	3.8	0.05
	8/1	2.4	−67.0		3.58×10^{-5}	9.63×10^{-6}	2.16×10^{-6}	3.5	0.09
	6/1	3.2	−62.0		6.70×10^{-6}	6.31×10^{-7}			

which only a single solvent (methanol) was used, showed the parent ions of both POSS-benzyl$_7$(BF$_3$Li)$_3$ and POSS-benzyl$_7$(BF$_3$Li)$_2$(Li) at 1151.2 and 1077.2, respectively. We did not try to separate this mixture, but the same batch of sample (which we will still refer to as POSS-benzyl$_7$(BF$_3$Li)$_3$) was used for all subsequent experiments. The addition of excess BF$_3$(OC$_2$H$_5$)$_2$ always yielded a mixture of POSS-benzyl$_7$(BF$_3$Li)$_3$ and POSS-benzyl$_7$(BF$_3$Li)$_2$, with the former the dominant species.

Calorimetric and conductivity data were obtained for mixtures of POSS-benzyl$_7$(BF$_3$Li)$_3$ and POSS-PEG$_8$ and compared with similar mixtures of POSS-benzyl$_7$Li$_3$/POSS-PEG$_8$ and LiBF$_4$/POSS-PEG$_8$ as a function of O/Li. A summary of all the calorimetric and conductivity data (90, 30, and 10 °C) is presented in Table I. DSC data can elucidate the degree of Li$^+$ dissociation for the electrolytes, because complexation of Li$^+$ with ethylene oxide (EO) units suppresses T_m and raises T_g.

DSC data, shown for electrolytes prepared with O/Li = 16/1, and plots of the glass transition temperature (T_g) versus O/Li (Figure 3) for POSS-benzyl$_7$(BF$_3$Li)$_3$/POSS-PEG$_8$, LiBF$_4$/POSS-PEG$_8$ and POSS-benzyl$_7$Li$_3$/POSS-PEG$_8$, highlight the effects of the type of salt and O/Li on T_g. The results demonstrate clearly the increased dissociation of the Li$^+$ in the POSS-benzyl$_7$(BF$_3$Li)$_3$/POSS-PEG$_8$ compared with that in LiBF$_4$/POSS-PEG$_8$ and in POSS-benzyl$_7$Li$_3$/POSS-PEG$_8$. The POSS-PEG$_8$ has a low T_g = −81 °C, as observed previously,[18] and there is a melt at T_m = −2 °C. The values of T_g and T_m more closely match a POSS-PEG$_8$ cage with 8 rather than 13.3 ethylene oxide units, but the disorder of the mixed arm lengths may decrease T_g and T_m.[18] The addition of salt decreases the enthalpy (ΔH_m) of the melting transition (i.e., decreases the percent crystallinity) in the order ΔH_m (POSS-benzyl$_7$(BF$_3$Li)$_3$/POSS-PEG$_8$) < ΔH_m (LiBF$_4$/POSS-PEG$_8$) < ΔH_m (POSS-benzyl$_7$Li$_3$/POSS-PEG$_8$) (Figure 3 top) and increases T_g in the order T_g (POSS-benzyl$_7$(BF$_3$Li)$_3$/POSS-PEG$_8$) > T_g(LiBF$_4$/POSS-PEG$_8$) > T_g (POSS-benzyl$_7$Li$_3$/POSS-PEG$_8$) for all O/Li (Figure 3 bottom and Table I). These trends support the view that more Li$^+$ ions dissociate for POSS-benzyl$_7$(BF$_3$Li)$_3$/POSS-PEG$_8$: the ions form complexes with the ether oxygens of PEG, increasing T_g and inhibiting crystallization. Further, as expected, T_g increases as O/Li decreases for POSS-benzyl$_7$(BF$_3$Li)$_3$/POSS-PEG$_8$, LiBF$_4$/POSS-PEG$_8$, and POSS-benzyl$_7$Li$_3$/POSS-PEG$_8$: in all cases, more Li$^+$ are available for complexation with POSS-PEG$_8$.

Conductivity plots for POSS-benzyl$_7$(BF$_3$Li)$_3$/POSS-PEG$_8$ as a function of the O/Li ratio are presented in Figure 4. Because the highest conductivity was measured for O/Li = 16/1, the conductivity data for the other two electrolytes, LiBF$_4$/POSS-PEG$_8$ and POSS-benzyl$_7$Li$_3$/POSS-PEG$_8$ at O/Li = 16/1 are shown for comparison. Consistent with the lack of crystallinity in any of the samples above 10 °C (Table I, Figure 3), there are no discontinuities in the plots resulting from the onset of crystallization, as is typically observed for PEO at ∼60 °C.

The conductivity of the POSS-benzyl$_7$(BF$_3$Li)$_3$/POSS-PEG$_8$ electrolyte is greater by a factor of 17, compared with LiBF$_4$/POSS-PEG$_8$, and by ∼50, compared with POSS-benzyl$_7$Li$_3$/POSS-PEG$_8$ at 30 °C (O/Li = 16/1), over the whole temperature range; the conductivity measured for the LiBF$_4$/POSS-PEG$_8$ is comparable to that observed previously.[19] The conductivities of the LiBF$_4$/POSS-PEG$_8$ and POSS-benzyl$_7$Li$_3$/POSS-PEG$_8$ are lower than those of the POSS-benzyl$_7$(BF$_3$Li)$_3$/POSS-PEG$_8$ despite the lower values of T_g for LiBF$_4$/POSS-PEG$_8$ and POSS-benzyl$_7$Li$_3$/POSS-PEG$_8$ at comparable O/Li ratios (Figures 3 and 4, Table I). This again indicates that the low T_g values reflect fewer dissociated Li$^+$ ions that can complex with the ether oxygens of the POSS-PEG$_8$. Although we did not measure the viscosity of these samples, the electrolytes prepared with LiBF$_4$ were always liquids (viscous) that flowed under their own weight. By contrast, the POSS-benzyl$_7$(BF$_3$Li)$_3$/POSS-PEG$_8$ and POSS-benzyl$_7$Li$_3$/POSS-PEG$_8$ did not flow under their own weight, and the POSS-benzyl$_7$(BF$_3$Li)$_3$ was stiffer than the POSS-PEG$_8$/POSS-benzyl$_7$Li$_3$. This suggests, as discussed below, that the morphology of the electrolytes is determined by the association of the phenyl rings of POSS.

dx.doi.org/10.1021/cm2015675 | Chem. Mater. XXXX, XXX, XXX−XXX

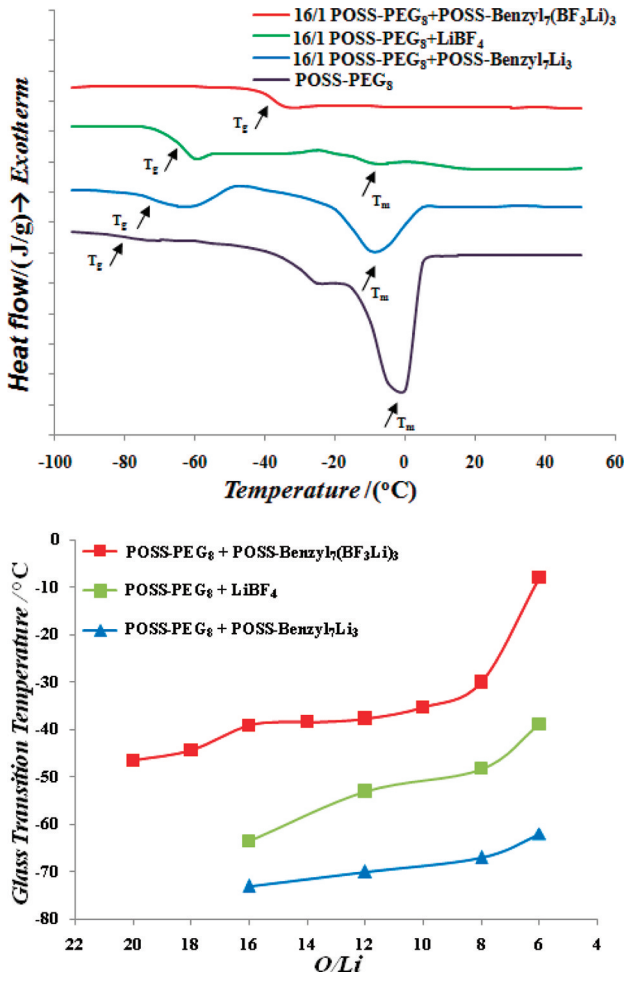

Figure 3. (top) DSC scans (second heating cycle) of POSS-PEG_8 and mixtures of POSS-benzyl$_7(BF_3Li)_3$)/POSS-PEG_8, $LiBF_4$/POSS-PEG_8, and (POSS-benzyl$_7Li_3$)/POSS-PEG_8 at O/Li = 16/1. T_g and T_m are indicated by arrows. (bottom) T_g versus O/Li for POSS-benzyl$_7(BF_3Li)_3$/POSS-PEG_8, $LiBF_4$/POSS-PEG_6, and (POSS-benzyl$_7Li_3$)/POSS-PEG_8.

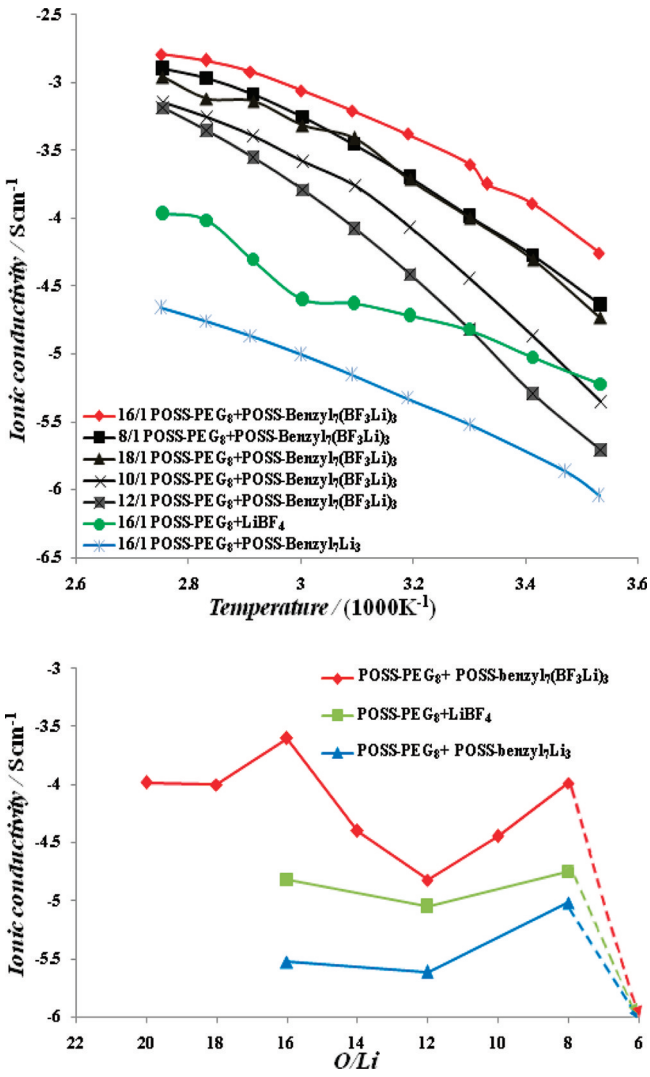

Figure 4. (top) Log conductivity(σ, S/cm) versus 1000/T for POSS-benzyl$_7(BF_3Li)_3$/POSS-PEG_8 as a function of the O/Li ratio, and for $LiBF_4$/POSS-PEG_8 and POSS-benzyl$_7Li_3$/POSS-PEG_8 at O/Li = 16/1; (bottom) log conductivity (σ, S/cm) versus O/Li for POSS-benzyl$_7(BF_3Li)_3$/POSS-PEG_8, $LiBF_4$/POSS-PEG_8 and POSS-benzyl$_7Li_3$/POSS-PEG_8 at 30 °C. Dotted lines for O/Li = 6/1 indicate that σ cannot be measured for these materials at 30 °C.

The increase in conductivity of one to two powers of ten, brought about by the replacement of −Si−O−Li by −Si−O−BF_3Li, is similar to that observed in polymer electrolyte gels[30,31] and in blends of PEO with poly(lithium carboxylate)s,[32,34] in which −COOLi was replaced by −COO BF_3Li. In the latter case, the increased conductivity, compared with the Li carboxylates, was attributed to the formation of a coordinate bond between the oxygen atom and boron atom, so that the lithium cations were separated from carboxylic acid anions, facilitating salt dissociation.[29] The ionic conductivity of solid polymer electrolytes composed of poly(ethylene oxide) (PEO) and poly(lithium carboxylate)s were enhanced by 1 or 2 orders of magnitude upon the addition of $BF_3(OC_2H_5)_2$, for the same reason, namely, that the dissociation of the Li^+ and the carboxylate anion was promoted by complexation with BF_3;[32] conversion of COO^-Li^+ to $COOBF_3^-Li^+$ in block copolymer SICs with BF_3 also resulted in increased Li^+ dissociation.[22]

In the current investigation, the large increase in conductivity was achieved not only at high temperatures but also at temperatures of 10 °C, because the POSS-benzyl$_7(BF_3Li)_3$ suppressed crystallization in the POSS-PEO_8. Further, the order of magnitude increase in conductivity for systems prepared with −Si−O−BF_3Li compared with $LiBF_4$ strongly implicates anion stabilization, which permits greater dissociation of the Li^+.

All of the conductivity plots exhibited Vogel−Tammann−Fulcher (VTF) behavior, for which

$$\sigma = AT^{-1/2} \exp[-E_a/k_B(T - T_0)] \quad (2)$$

suggesting that the Li^+ transport is coupled to the segmental relaxation of the POSS-PEG_8 and that the POSS-PEG_8 therefore behaves like a polymer matrix. The decomposition temperature (T_d) for POSS-PEG_8 (388 °C) was in the range observed for high molecular weight PEO in N_2,[35,36] consistent with the idea that the aggregate of PEG chains behaved similarly to PEO. In this equation, A is a pre-exponential factor proportional to the number of charge carriers, E_a is the pseudo-activation energy for ionic conductivity, and T_0 is a reference temperature, at which the free volume disappears (approximately T_g − 50 °C) so that molecular motion is frozen out (i.e., the relaxation times in the polymer electrolyte become

dx.doi.org/10.1021/cm2015675|Chem. Mater. XXXX, XXX, XXX−XXX

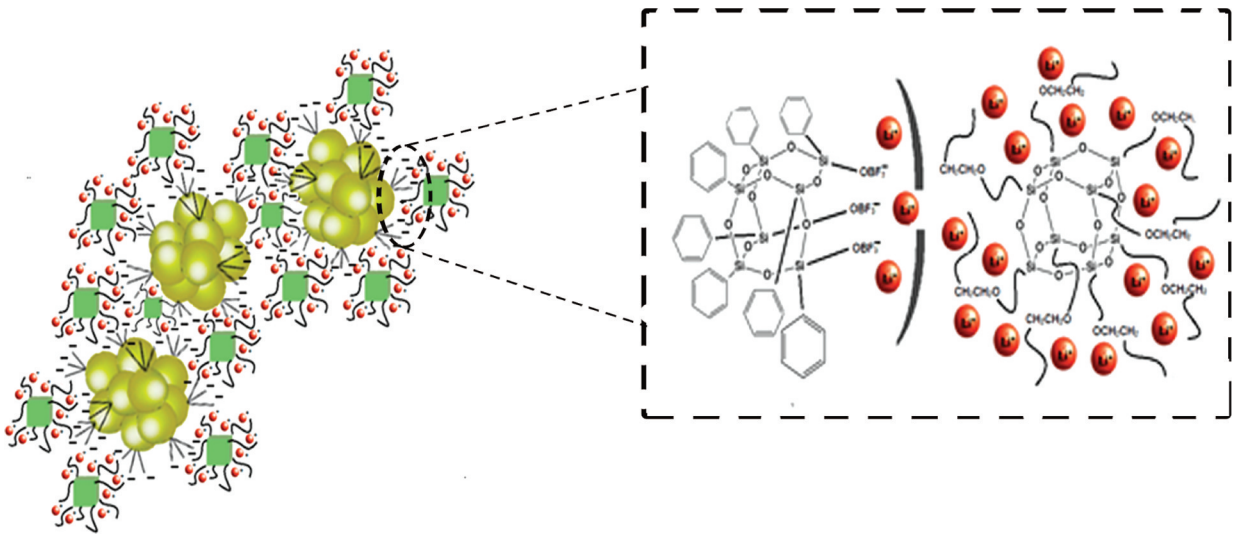

Figure 5. Schematic of the two phase structure of POSS-benzyl$_7$(BF$_3$Li)$_3$/POSS-PEG$_8$: (i) one phase is clustered phenyl groups with POSS-benzyl$_7$(BF$_3$)$_3^{3-}$ anions oriented outward; (ii) the other phase is POSS-PEG$_8$ with solvated Li$^+$. Inset shows a schematic of the phase boundary.

infinite). The activation energies and values of A calculated from the VTF equation (eq 2), using experimental T_g values, are presented in Table I.

E_a varied from 2.8 to 4.7 kJ/mol (average ca. 3.8 ± 0.5 kJ/mol) for all the samples. The lowest value of E_a (2.8 kJ/mol) was obtained for POSS-benzyl$_7$(BF$_3$Li)$_3$/POSS-PEG$_8$ (O/Li = 16/1), which also exhibited the highest conductivity. These values are typical for liquid (3−6 kJ/mol),[37−39] including low molecular weight PEG, electrolytes (5−7 kJ/mol),[40−42] but not for polymer-gel[43] or high molecular weight PEO-based polymer electrolytes (20−75 kJ/mol),[44−46] or ones with PEG side chains[47] or PEG blocks[48] (8−13 kJ/mol). We previously obtained values of ca. 12 kJ/mol for POSS-PEG$_8$ with various lithium salts,[20] and the lower values now measured may result from the longer but more disordered PEG side-chains.

Values of A calculated from the VTF equation, using experimental T_g values (Table I) increase in the order A(POSS-benzyl$_7$(BF$_3$Li)$_3$/POSS-PEG$_8$) > A(LiBF$_4$/POSS-PEG$_8$) ≫ A(POSS-benzyl$_7$Li$_3$/POSS-PEG$_8$), indicating that dissociation of the Li$^+$ is greatest for the POSS-benzyl$_7$(BF$_3$Li)$_3$ and very weak for the POSS-benzyl$_7$Li$_3$, in agreement with both the DSC and σ data. A was highest for POSS-benzyl$_7$(BF$_3$Li)$_3$/POSS-PEG$_8$ (O/Li = 16/1), which also exhibited the highest conductivity.

To further understand the conductivity trends for the electrolyte of interest, POSS-benzyl$_7$(BF$_3$Li)$_3$, conductivities (eg at 30 °C) can be compared as a function of O/Li (Figure 4 bottom, Table I). It should be noted that the conductivity first increases with decreasing O/Li ratio, as more Li$^+$s are introduced, as expected. A maximum is reached at O/Li = 16/1, followed by a decrease with decreasing O/Li ratio. Since T_g also increases with decreasing O/Li ratio, this maxima is often explained as a competition between two affects, namely, an increase in charge carriers and a decrease in mobility with decreasing O/Li ratio. An interesting feature in the data is that the conductivity then begins to increase again with decreasing O/Li ratio, despite the increase in T_g, and then, it drops again; at O/Li = 6/1, σ measurements cannot be made at RT. The conductivity is only half as high at O/Li = 8/1 as at is at 16/1. The maximum at O/Li = 8/1 suggests that it is possible to further increase the number density of the mobile ion species in this system. Two maxima have previously been observed in other amorphous PEO based systems.[49,50] We speculate that the second maximum in conductivity at O/Li = 8/1 arises due to the structure of the POSS-benzyl$_7$(BF$_3$Li)$_3$: (i) it has a large anion to stabilize the negative charge;[51] (ii) the Janus-like nature orients the molecule so that the −Si−O−BF$_3^-$ groups point toward the POSS-PEG$_8$; and (iii) the benzyl groups cluster and prevent formation of triplets.

The subsequent decrease in conductivity (at O/Li = 6/1) is due both to the increase in T_g and to a proposed two-phase morphology for this system: there is a structural phase that consists of clusters of phenyl groups with Si−O−BF$_3^-$ anions and a conductive phase that consists of POSS-PEG$_8$ with associated Li$^+$ cations, as presented schematically in Figure 5. We attribute the precipitous drop in conductivity at O/Li = 6/1 (σ cannot be measured below 70 °C) to the elimination of a conductive path for the POSS-PEG$_8$ phase as the phenyl groups crystallize. If it is assumed that the densities of the POSS-benzyl$_7$(BF$_3$Li)$_3$ and POSS-PEG$_8$ are similar, then a system in which the Li$^+$/POSS-PEG$_8$ forms one phase and the POSS-benzyl$_7$(BF$_3$)$_3^{3-}$ forms the second phase would be expected to be cocontinuous phases approximately at a 50/50 weight ratio. This would occur at ca. O/Li = 8/1 to 6/1. Thus for the O/Li = 6/1, only the POSS-benzyl$_7$(BF$_3$)$_3^{3-}$ phase would be continuous. The Li$^+$/POSS-PEG$_8$ would form nonconnected microphase separated domains within this structure, resulting in low ionic conductivities.

Evidence of two phases, which we associate with clustering of the phenyl portion of the POSS-benzyl$_7$(BF$_3$)$^{3-}$ is seen both visually and by DSC. At a temperature above ∼80 °C, the electrolyte is clear and transparent, but it becomes opaque at room temperature. This change in appearance coincides with what appears very much like a crystallization transition with a crystallization temperature (T_c) between 30 and 70 °C (Figure 6) and a crystallization enthalpy of 47.5 J/g. Modulated DSC confirmed that this was, in fact, crystallization and not a T_g. The transition was observed when freshly prepared POSS-benzyl$_7$(BF$_3$Li)$_3$/POSS-PEG$_8$ (at 90 °C) was directly placed in the DSC, heated quickly to 120 °C and then cooled. When reheated to 90 °C, it took ∼3 h before the system again looked

dx.doi.org/10.1021/cm2015675 | Chem. Mater. XXXX, XXX, XXX−XXX

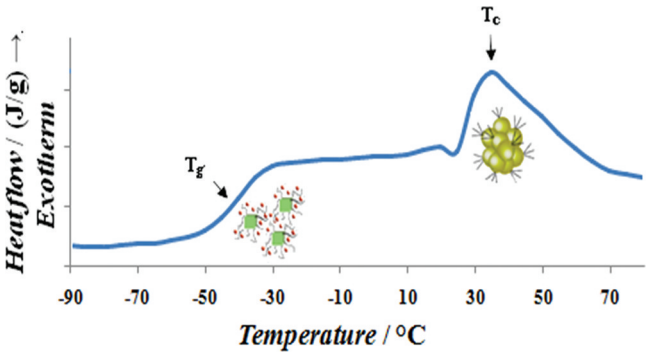

Figure 6. DSC cooling cycle (5 °C/min) of POSS-benzyl$_7$(BF$_3$Li)$_3$/POSS-PEG$_8$ (O/Li = 16/1) showing crystallization exotherm (from clustering of phenyl groups of POSS-benzyl$_7$(BF$_3$)$_3^{-3}$), not PEO crystallization, and T_g from POSS-PEG$_8$ solvated with Li$^+$.

transparent; the exotherm then appeared on the subsequent cooling cycle. This suggests that the phenyl aggregates in the POSS-benzyl$_7$(BF$_3$)$_3^{3-}$ domains do not melt abruptly and take time to dissociate.

The assignment of these transitions (to clustering of the phenyl portions of the POSS-benzyl$_7$(BF$_3$)$^{3-}$ is done because they did not occur for the POSS-PEG$_8$/LiBF$_4$ and, in analogy with similar clustering of POSS in incompatible POSS/polymer systems such as polyurethane-POSS,[52] ABA triblock copolymers[53] and polyethylene (PE)-POSS copolymers.[54,55] For the PE-POSS systems, both components were crystalline, and therefore, they exhibited two crystallization peaks below T_m of the PE; however, in the melt (above T_m of PE), there were POSS domains. Replacement of semicrystalline PE with the amorphous, low T_g polybutadiene allowed better mobility of the POSS (because the crystallization of PE was not a competitive process) and therefore better self-assembly of two-dimensional POSS domains.[56] No DSC transitions (to 400 °C) were associated with the POSS crystals observed by WAXS (wide angle X-ray scattering) and SAXS (small angle X-ray scattering) experiments.[56] It was shown in ethylene-propylene-silsesquioxane elastomers that the restraints of covalent attachment of incompatible POSS (with phenyl groups) permitted only 2-D organization, with the crystallites acting as cross-link sites; mixing of compatible POSS (with isobutyl and ethyl groups) resulted in the dispersion of the POSS.[57] In the case of POSS-PEG telechelic copolymers (with POSS moieties attached to both ends of PEO), an order−disorder transition was observed; at low temperature, there were two crystalline domains (PEO and POSS), and at higher temperature, the material was rubbery due to POSS cross-linking, and at yet higher temperature, the material exhibited viscous liquid-like behavior.[58]

In the current investigation, both components, POSS-PEG$_8$ and POSS-benzyl$_7$(BF$_3$Li)$_3$ were amorphous; the former was a viscous liquid, and the latter was an amorphous solid, possibly due to the use of a sample composed of predominantly POSS-benzyl$_7$(BF$_3$Li)$_3$ but some POSS-benzyl$_7$(BF$_3$Li)$_2$Li. Furthermore, here, the POSS-PEG$_8$ and POSS-benzyl$_7$(BF$_3$Li)$_3$ existed as separate nanoparticles and were not covalently linked, as in the systems described above. However, the interactions between the phenyl groups in POSS-benzyl$_7$(BF$_3$Li)$_3$ were not sufficiently strong to form a solid structure, only a very viscous liquid that did not flow under its own weight.

The larger anion (POSS-benzyl$_7$(BF$_3$)$_3^{-3}$) compared with BF$_4^-$ suggests that more of the charge should be carried by the Li$^+$ for the POSS-benzyl$_7$(BF$_3$Li)$_3$ system. Figure 7 shows an example of the time dependent decrease in current (I) that occurred after a DC polarization pulse of 50 mV and the Cole−Cole impedance spectra obtained initially (I_0) and at the steady state (I_{ss}) value for POSS-PEG$_8$/POSS-benzyl$_7$(BF$_3$Li)$_3$ with O/Li = 16/1, at 80 °C. The measurements were performed after the establishment of a stable solid electrolyte interface (SEI layer). The value of the lithium ion transference number obtained from this data (eq 1) was $t_{Li^+} = 0.50 \pm 0.01$, where the standard deviation was obtained from three measurements.

The interfacial properties of the lithium anode in contact with the POSS-benzyl$_7$(BF$_3$Li)$_3$/POSS-PEG$_8$ were measured from Cole−Cole impedance spectra, obtained using lithium electrodes. The plots, measured under open circuit conditions, for the nanocomposite that exhibited the highest ionic

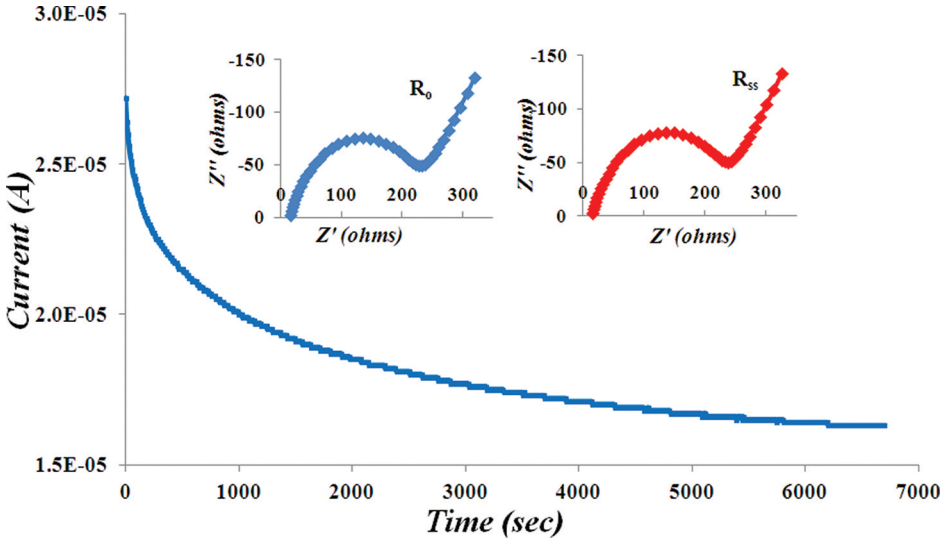

Figure 7. Variation of current (I) with time during polarization of a Li^0/POSS-benzyl$_7$(BF$_3$Li)$_3$/POSS-PEG$_8$ (O/Li = 16/1)/Li^0 cell at 80 °C, with an applied potential difference of 10 mV. Inset shows Cole−Cole plots taken initially (I_0) and when the current had reached the steady state value (I_{ss}).

dx.doi.org/10.1021/cm2015675 | Chem. Mater. XXXX, XXX, XXX−XXX

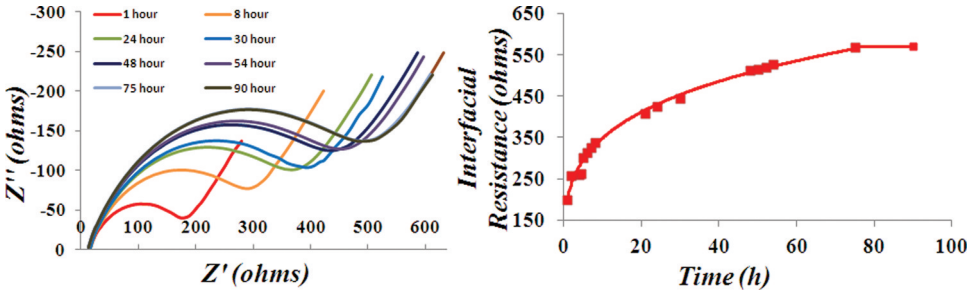

Figure 8. (left) Select impedance (Cole–Cole) plots of a Li^0/POSS-benzyl$_7$(BF_3Li)$_3$/POSS-PEG_8 (O/Li = 16/1)/Li^0 cell (open circuit potential) as a function of storage time at 80 °C; (right) Interfacial resistance as a function of storage time at 80 °C.

conductivity (O/Li = 16/1) are shown in Figure 8, left, as a function of storage time. The diameters of the spectra, which are semicircles with a slanted line at low frequency, increase with storage time and finally stabilize. The intercept at high frequency has been modeled as the ohmic resistance of the cell, due mainly to the electrolyte resistance (R_{bulk}), and does not change with storage time (13 Ω). The low frequency intercept, taken as the value of the slanted line extraplolated to the R′ axis, increases with storage time and stabilizes after ∼3 days (Figure 8 right) to a value of ∼550 Ω. The diameter of the semicircle has contributions from both the resistance of the passivation film ($R_{passivation}$), first observed in solid polymer electrolytes for PEO/$LiCF_3SO_3$,[59] and the charge-transfer resistance (R_{CT});[27] R_{CT} can also occur as a smaller (sometimes poorly resolved) semicircle at lower frequency.[60] The stabilization of this resistance suggests that the film formed at the polymer electrolyte interface has good passivation characteristics, as has been observed upon the addition of ceramic nanofillers to PEO.[9]

To determine if a solid could be formed, we added polystyrene (PS) or PS-*b*-PEO (to compatibilize the POSS-PEG_8 and the PS). The addition of PS or PS-*b*-PEO, under conditions in which the Li^+/POSS-PEG_8 was the minor phase (O/Li = 8/1), did form a nonconductive solid, in which the T_g was the same as for POSS-benzyl$_7$(BF_3Li)$_3$/POSS-PEG_8. This strongly suggested that there were nonconnected pockets of the conductive phase, with the phenyl groups associating with the PS and the Si–O–BF_3^- pointing toward the Li^+/POSS-PEG_8 phase. The addition of small amounts of PEO, or PEO itself, could be used to form a SPE without PEO crystallization (using this POSS-benzyl$_7$(BF_3Li)$_3$ salt). The conductivities and transference numbers of systems with PEO or PEO/POSS-PEG_8 were $\sigma > 1 \times 10^{-4}$ and $t_{Li^+} > 0.5$, respectively, and will be reported separately.

The thermal degradation of the electrolytes was investigated by TGA, with the results shown in Figure 9 for the separate materials and their mixtures. The calculated weight loss for the C and H versus Si, O, and Li components agreed reasonably well with the experimental results. For POSS-PEG_8, the maximum rate of weight loss was at 388 °C, but the sample degrades over a broad temperature range. This degradation temperature is in the range of the degradation temperatures observed for high molecular weight PEO in N_2, consistent with the idea that the aggregate of chains behave similarly to PEO. Previous work for POSS-PEG_8 with m = 2, 3, and 6 suggests that degradation temperature increases are enhanced for ethylene oxide segments close to the $SiO_{1.5}$ cage,[36] and PEO segments directly adsorbed onto SiO_2 nanoparticles exhibited higher T_d.[35] For the POSS-benzyl$_7$(BF_3Li)$_3$, there were two

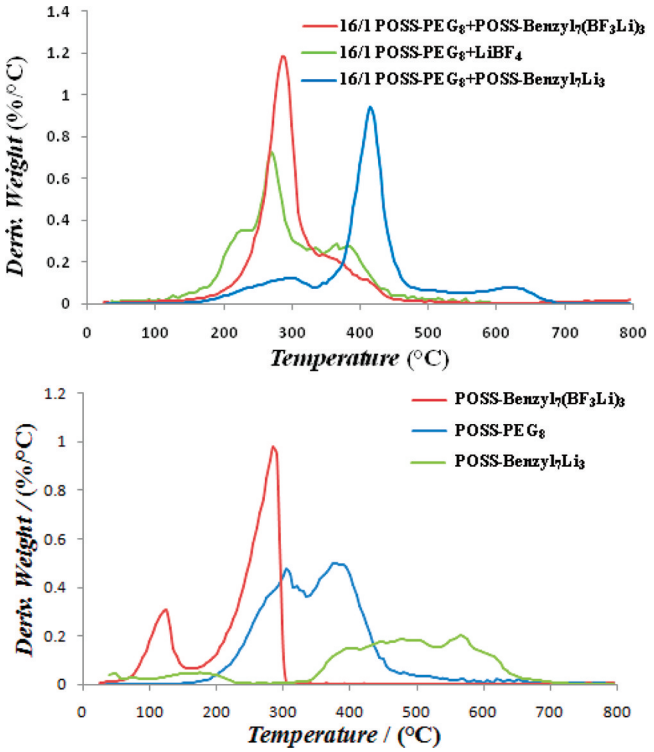

Figure 9. (bottom) Deriviative weight loss (dTGA) plots for POSS-PEG_8, POSS-benzyl$_7$$Li_3$ and POSS-benzyl$_7$(BF_3Li)$_3$; (top) dTGA plots for mixtures of POSS-PEG_8 with POSS-benzyl$_7$(BF_3Li)$_3$, $LiBF_4$ and POSS-benzyl$_7$$Li_3$, at O/Li = 16/1.

distinct narrow weight loss steps, one with a maximum rate of weight loss at 123 °C, and the other with a maximum rate of weight loss at 286.5 °C. The first can be attributed to the loss of the BF_3 and the second to degradation of the organic phenyl groups. In the O/Li = 16/1 composite electrolytes, the degradation is composed approximately of the contributions of the two components. For the POSS-PEG_8/POSS-benzyl$_7$(BF_3Li)$_3$, the main degradation peak for the composite was narrow and coincided with the degradation of the POSS-benzyl$_7$(BF_3Li)$_3$ (288 °C), with a smaller peak at the same position as pure POSS-PEG_8 (360 °C).

In the case of POSS-PEG_8/POSS-benzyl$_7$$Li_3$ and POSS-PEG_8/POSS-benzyl$_7$(BF_3Li)$_3$, the material remaining in the TGA pan is a black char, while for the POSS-PEG_8/$LiBF_4$, the material was not charred. This indicates that, as previously reported for metal containing POSS,[61,62] POSS-benzyl$_7$(BF_3Li)$_3$ and POSS-PEG_8/POSS-benzyl$_7$$Li_3$ may have fire retardant properties. Incorporation of POSS has been shown to enhance thermal and oxidative stability, as well as flammability

dx.doi.org/10.1021/cm2015675 | Chem. Mater. XXXX, XXX, XXX–XXX

resistance, largely as a result of the inorganic $SiO_{1.5}$ core.[63] In general, the greater the amount of POSS[64] and the better dispersed the nanoparticle filler,[65,66] the greater the capability of reducing the peak heat release rate (HRR) and time to ignition (TI). The improved fire retardancy and oxidative stability of POSS are brought about by two primary mechanisms: (i) they have reduced volatility (exhibit no appreciable vapor pressures) due to their high molar mass, and they also reduce the volatilization of the organic monomer/polymer components, and (ii) they form oxidatively stable, nonpermeable inorganic surface chars that are fire resistant and passivate surfaces.[67] Inorganic salts generally reduce the thermal stability of PEO in an inert atmosphere but protect the polymer against thermal oxidation.[68]

CONCLUSIONS

Hybrid polyoctahedral silsesquioxane (POSS)-based electrolyes have been prepared from POSS-PEG_8 and POSS-benzyl$_7$(BF_3Li)$_3$. The latter were synthesized by reaction of POSS-benzyl$_7$Li$_3$ with $BF_3(OC_2H_5)_2$. The resulting salt had a stable, electron withdrawing anion that enabled facile dissociation of the Li cation. The Li^+ was solvated by the ethylene oxide units of POSS-PEG_8, raising T_g and improving conductivity of the nanomaterial compared with POSS-benzyl$_7$Li$_3$ and $LiBF_4$ at the same O/Li ratios. The lithium ion transference number, t_{Li^+} was 0.50 ± 0.01, due to reduced mobility of the large bulky anion. Of importance was that the increased t_{Li^+} occurred simultaneously with enhanced conductivity. This was associated with the Janus-like behavior of the POSS-benzyl$_7$(BF_3Li)$_3$, with one end ionic and the remainder hydrophobic as a result of the attached phenyl groups. The phenyl groups interacted and aggregated into hydrophobic clusters as evidenced by a crystallization exotherm. The proposed morphology of these nanomaterials was one in which there were both hydrophobic domains consisting of phenyl rich POSS, with the $-Si-O-BF_3^-$ pointing toward the hydrophilic POSS-PEG_8 domains that solvated the Li^+ cation. While the POSS-PEG_8/POSS-benzyl$_7$(BF_3Li)$_3$ mixtures were still only very viscous materials that did not flow under their own weight, the addition of small amounts of high molecular weight PEO yielded solid materials with comparable conductivities.

ASSOCIATED CONTENT

Supporting Information

Table of solubilities for POSS-benzyl$_7$Li$_3$, POSS-benzyl$_7$(BF_3Li)$_3$, POSS-PEG_8, and octaphenyl-POSS in solvents with different solubility parameters. This material is available free of charge via the Internet at http://pubs.acs.org.

AUTHOR INFORMATION

Corresponding Author

*E-mail: slwunder@temple.edu.

ACKNOWLEDGMENTS

We wish to thank Gopal Sirasani for help with synthesis of POSS-benzyl$_7$(BF_3Li)$_3$, Jayvic Jimenez for assistance with preparation of the figures, Sahithi Mudigonda with help acquiring the conductivity data, Charles de Brosse for NMR data, and Hybrid Plastics/ONR-SBIR for the donation of starting materials and financial support.

REFERENCES

(1) Tarascon, J. M. *Philos. Trans. R. Soc., A* **2010**, *368* (1923), 3227–3241.
(2) Armand, M.; Tarascon, J. M. *Nature* **2008**, *451* (7179), 652–657.
(3) Bruce, P. G. *Solid State Ionics* **2008**, *179* (21–26), 752–760.
(4) *Polymer Electrolyte Reviews*; MacCallum, J. R., Vincent, C. A., Eds.; Elsevier: Amsterdam, 1987; Vol. *1*.
(5) Booth, C.; Nicholas, C. V.; Wilson, D. J. In *Polymer Electrolyte Reviews*; MacCallum, J. R., Vincent, C. A., Eds.; Elsevier: London, 1989; Vol. *2*, Chapter 7.
(6) Gray, F. M. *Polymer Electrolytes*; The Royal Society of Chemistry: Cambridge, 1997.
(7) Gray, F. M. *Solid Polymer Electrolytes—Fundamentals and Technical Applications*; VCH: Wenheim, 1991.
(8) Croce, F.; Appetecchi, G. B.; Persi, L.; Scrosati, B. *Nature* **1998**, *394*, 456–458.
(9) Croce, F.; Curini, R.; Martinelli, A.; Persi, L.; Ronci, F.; Scrosati, B.; Caminiti, R. *J. Phys. Chem. B* **1999**, *103* (48), 10632–10638.
(10) Bruce, P. G.; Scrosati, B.; Tarascon, J. M. *Angew. Chem., Int. Ed.* **2008**, *47* (16), 2930–2946.
(11) Zhang, H. J.; Maitra, P.; Wunder, S. L. *Solid State Ionics* **2008**, *178* (39–40), 1975–1983.
(12) Kerr, J. B. Lithium Batteries. In *Science and Technology*, Nazri, G. A., Pistoia, G., Eds.; Kluwer Academic: Dordrecht, 2003; p 602.
(13) Armand, M.; Endres, F.; MacFarlane, D. R.; Ohno, H.; Scrosati, B. *Nat. Mater.* **2009**, *8* (8), 621–629.
(14) Lewandowski, A.; Swiderska-Mocek, A. *J. Power Sources* **2009**, *194* (2), 601–609.
(15) Moganty, S. S.; Jayaprakash, N.; Nugent, J. L.; Shen, J.; Archer, L. A. *Angew. Chem., Int. Ed.* **2010**, *49* (48), 9158–9161.
(16) Tanaka, K.; Ishiguro, F.; Chujo, Y. *J. Am. Chem. Soc.* **2010**, *132*, 17649–17651.
(17) Nugent, J. L.; Moganty, S. S.; Archer, L. A. *Adv. Mater.* **2010**, *22* (33), 3677–+.
(18) Maitra, P.; Wunder, S. L. *Chem. Mater.* **2002**, *14* (11), 4494–4497.
(19) Maitra, P.; Wunder, S. L. *Electrochem. Solid State Lett.* **2004**, *7* (4), A88–A92.
(20) Zhang, H. J.; Kulkarni, S.; Wunder, S. L. *J. Electrochem. Soc.* **2006**, *153* (2), A239–A248.
(21) Sadoway, D. R.; Huang, B. Y.; Trapa, P. E.; Soo, P. P.; Bannerjee, P.; Mayes, A. M. *J. Power Sources* **2001**, *97–8*, 621–623.
(22) Ryu, S. W.; Trapa, P. E.; Olugebefola, S. C.; Gonzalez-Leon, J. A.; Sadoway, D. R.; Mayes, A. M. *J. Electrochem. Soc.* **2005**, *152* (1), A158–A163.
(23) Laine, R. M.; Roll, M.; Asuncion, M.; Sulaiman, S.; Popova, V.; Bartz, D.; Krug, D. J.; Mutin, P. H. *J. Sol–Gel Sci. Technol.* **2008**, *46* (3), 335–347.
(24) Bassindale, A. R.; Chen, H. P.; Liu, Z. H.; MacKinnon, L. A.; Parker, D. J.; Taylor, P. G.; Yang, Y. X.; Light, M. E.; Horton, P. N.; Hursthouse, M. B. *J. Organomet. Chem.* **2004**, *689* (21), 3287–3300.
(25) Bassindale, A. R.; Liu, Z. H.; Taylor, P. G.; Horton, P. N.; Hursthouse, M. B. *Chem. Commun.* **2008**, *43*, 5625–5627.
(26) Evans, J.; Vincent, C. A.; Bruce, P. G. *Polymer* **1987**, *28* (13), 2324–8.
(27) Abraham, K. M.; Jiang, Z.; Carroll, B. *Chem. Mater.* **1997**, *9* (9), 1978–1988.
(28) Zhang, H. J.; Kulkarni, S.; Wunder, S. L. *J. Phys. Chem. B* **2007**, *111* (14), 3583–3590.
(29) Florjanczyk, Z.; Bzducha, W.; Dygas, J. R.; Misztal-Faraj, B.; Krok, F. *Solid State Ionics* **1999**, *119* (1–4), 251–259.
(30) Florjanczyk, Z.; Bzducha, W.; Langwald, N.; Dygas, J. R.; Krok, F.; Misztal-Faraj, B. *Electrochim. Acta* **2000**, *45* (21), 3563–3571.
(31) Kang, W. C.; Park, H. G.; Kim, K. C.; Ryu, S. W. *Electrochim. Acta* **2009**, *54* (19), 4540–4544.
(32) Itoh, T.; Yoshikawa, M.; Uno, T.; Kubo, M. *Ionics* **2009**, *15* (1), 27–33.

(33) Asuncion, M. Z.; Ronchi, M.; Abu-Seir, H.; Laine, R. M. *C. R. Chim.* **2010**, *13* (1−2), 270−281.
(34) Itoh, T.; Mitsuda, Y.; Ebina, T.; Uno, T.; Kubo, M. *J. Power Sources* **2009**, *189* (1), 531−535.
(35) Madathingal, R. R.; Wunder, S. L., Thermal degradation of PEO on SiO_2 Nanoparticles as a function of SiO_2 silanol density, hydrophobicity and size. *Thermochim. Acta* **2011**, accepted for publication.
(36) Markovic, E.; Ginic-Markovic, M.; Clarke, S.; Matisons, J.; Hussain, M.; Simon, G. P. *Macromolecules* **2007**, *40* (8), 2694−2701.
(37) Ding, M. S.; Jow, T. R. *J. Electrochem. Soc.* **2003**, *150* (5), A620−A628.
(38) Ding, M. S. *J. Electrochem. Soc.* **2004**, *151* (1), A40−A47.
(39) Ding, M. S.; Xu, K.; Jow, T. R. *J. Electrochem. Soc.* **2005**, *152* (1), A132−A140.
(40) Hayamizu, K.; Akiba, E.; Bando, T.; Aihara, Y. *J. Phys. Chem.* **2002**, *117* (12), 5929−5939.
(41) Johansson, A.; Gogoll, A.; Tegenfeldt, J. *Polymer* **1996**, *37* (8), 1387−1393.
(42) Paillard, E.; Iojoiu, C.; Alloin, F.; Guindet, J.; Sanchez, J. Y. *Electrochim. Acta* **2007**, *52* (11), 3758−3765.
(43) Aihara, Y.; Appetecchi, G. B.; Scrosati, B. *J. Electrochem. Soc.* **2002**, *149* (7), A849−A854.
(44) Appetecchi, G. B.; Dautzenberg, G.; Scrosati, B. *J. Electrochem. Soc.* **1996**, *143* (1), 6−12.
(45) Koksbang, R.; Olsen, I. I.; Shackle, D. *Solid State Ionics* **1994**, *69*, 320−335.
(46) Appetecchi, G. B.; Henderson, W.; Villano, P.; Berrettoni, M.; Passerini, S. *J. Electrochem. Soc.* **2001**, *148* (10), A1171−A1178.
(47) Soo, P. P.; Huang, B.; Jang, Y.-I.; Chiang, Y.-M.; Sadoway, D. R.; Mayes, A. M. *J. Electrochem. Soc.* **1999**, *146* (1), 32−37.
(48) Alloin, F.; Sanchez, J.-Y.; Armand, M. *J. Electrochem. Soc.* **1994**, *141* (7), 1915−1920.
(49) Sylla, S.; Sanchez, J. Y.; Armand, M. *Electrochim. Acta* **1992**, *37* (9), 1699−1701.
(50) Benrabah, D.; Baril, D.; Sanchez, J. Y.; Armand, M.; Gard, G. G. *J. Chem. Soc., Faraday Trans.* **1993**, *89* (2), 355−359.
(51) Tokuda, H.; Tabata, S. I.; Susan, M.; Hayamizu, K.; Watanabe, M. *J. Phys. Chem. B* **2004**, *108* (32), 11995−12002.
(52) Fu, B. X.; Hsiao, B. S.; Pagola, S.; Stephens, P.; White, H.; Rafailovich, M.; Sokolov, J.; Mather, P. T.; Jeon, H. G.; Phillips, S.; Lichtenhan, J.; Schwab, J. *Polymer* **2001**, *42* (2), 599−611.
(53) Pyun, J.; Matyjaszewski, K.; Wu, J.; Kim, G. M.; Chun, S. B.; Mather, P. T. *Polymer* **2003**, *44* (9), 2739−2750.
(54) Waddon, A. J.; Zheng, L.; Farris, R. J.; Coughlin, E. B. *Nano Lett.* **2002**, *2* (10), 1149−1155.
(55) Zheng, L.; Waddon, A. J.; Farris, R. J.; Coughlin, E. B. *Macromolecules* **2002**, *35* (6), 2375−2379.
(56) Zheng, L.; Hong, S.; Cardoen, G.; Burgaz, E.; Gido, S. P.; Coughlin, E. B. *Macromolecules* **2004**, *37* (23), 8606−8611.
(57) Seurer, B.; Coughlin, E. B. *Macromol. Chem. Phys.* **2008**, *209* (12), 1198−1209.
(58) Kim, B. S.; Mather, P. T. *Macromolecules* **2006**, *39* (26), 9253−9260.
(59) Fauteux, D. *Solid State Ionics* **1985**, *17* (2), 133−138.
(60) Alamgir, M.; Abraham, K. M. *J. Power Sources* **1995**, *54* (1), 40−45.
(61) Fina, A.; Bocchini, S.; Camino, G. In *Catalytic Fire Retardant Nanocomposites*, 2008; pp 1647−1655.
(62) Fina, A.; Abbenhuis, H. C. L.; Tabuani, D.; Camino, G. *Polym. Degrad. Stab.* **2006**, *91* (10), 2275−2281.
(63) Lichtenhan, J. D. Polyhedral oligomeric silsesquioxane flame retardancy. In *Industry Guide to Polymer Nanocomposites*; Beyer, G., Ed. Applied Market Information, LLC: Wyomissing, PA, 2009; Chapter 8.
(64) Jash, P.; Wilkie, C. A. *Polym. Degrad. Stab.* **2005**, *88* (3), 401−406.
(65) Bourbigot, S.; Duquesne, S.; Jama, C. *Macromol. Symp.* **2006**, *233* (1), 180−190.
(66) Bourbigot, S.; Duquesne, S.; Fontaine, G.; Bellayer, S.; Turf, T.; Samyn, F. *Molec. Cryst. Liquid Cryst.* **2008**, 1367−1381.
(67) Mantz, R. A.; Jones, P. F.; Chaffee, K. P.; Lichtenhan, J. D.; Gilman, J. W.; Ismail, I. M. K.; Burmeister, M. J. *Chem. Mater.* **1996**, *8* (6), 1250−1259.
(68) Costa, L.; Gad, A. M.; Camino, G.; Cameron, G. G.; Qureshi, M. Y. *Macromolecules* **1992**, *25* (20), 5512−5518.